
Tribology Transactions

ISSN: 1040-2004 (Print) 1547-397X (Online) Journal homepage: https://www.tandfonline.com/loi/utrb20

# Modeling Wear State Evolution Using Real-Time Wear Debris Features

Shuo Wang, Tonghai Wu, Hongkun Wu & Ngaiming Kwok

**To cite this article:** Shuo Wang, Tonghai Wu, Hongkun Wu & Ngaiming Kwok (2017) Modeling Wear State Evolution Using Real-Time Wear Debris Features, Tribology Transactions, 60:6, 1022-1032, DOI: 10.1080/10402004.2016.1243746

**To link to this article:** https://doi.org/10.1080/10402004.2016.1243746

Accepted author version posted online: 04 Oct 2016.
Published online: 18 Dec 2016.

TRIBOLOGY TRANSACTIONS
2017, VOL. 60, NO. 6, 1022–1032
https://doi.org/10.1080/10402004.2016.1243746

# Modeling Wear State Evolution Using Real-Time Wear Debris Features

Shuo Wang[a], Tonghai Wu[a], Hongkun Wu[b], and Ngaiming Kwok[b]

[a]Key Laboratory of Education Ministry for Modern Design and Rotor–Bearing System, Xi'an Jiaotong University, Xi'an, P. R. China; [b]School of Mechanical and Manufacturing Engineering, the University of New South Wales, Sydney, Australia

**ABSTRACT**
Because wear is one of the most typical causes of decreasing performance in running machines, monitoring wear is regarded as a crucial technology in maintaining the health of machines. However, monitoring wear is not a fully mature process because quantifying the development of wear in real time is a challenging task because there is no universal indicator. To meet this need, wear-oriented dynamic modeling with online ferrographic images was used to investigate and then describe a real-time wear state. This investigation was carried out by combining three wear indices to describe the wear rate, the wear mechanism, and the severity of wear. A binary classifier method is also proposed to classify these wear stages in the three extracted indices. A strategy to identify the dynamic transition of wear states with adaptive parameters is also developed and then a four-ball wear test is carried out to verify the method. The results indicate that this modeling strategy can accurately identify a developing wear state that is characterized by stages. This proposed method is better at monitoring the health evolution of a machine system than just detecting faults.

**ARTICLE HISTORY**
Received 17 March 2016
Accepted 27 September 2016

**KEYWORDS**
Dynamic modeling; equipment wear tests; wear particle analysis; oil condition monitoring

## Introduction

Wear-induced failure is a principle fault of running machines. It is mostly introduced by deterioration of wear performance and therefore can be reflected by their service condition indicators and general monitoring. In essence, the wear of mechanical triboparts is a dynamic and gradual process that passes through distinct stages from normal to failure. Good evidence for this general wear principle can be seen in a bathtub-shaped curve that shows how a typical wear process proceeds from a mild stage to a normal stage and then to a severe stage during the life span of a machine (Kothamasu, et al. *(1)*). Because these transitions in wear states are induced by alternating microwear mechanisms, a deteriorating wear performance can be inferred by investigating the transitions of mechanism related information. However, considering that online monitoring is mostly conducted without human activity, it is crucial to have reliable and quantitative wear states in order to conduct a lifetime and real-time evaluation of machine health, as well as a failure diagnosis and prognosis.

Condition monitoring based on wear is a practical way of obtaining information on wear but, unlike vibration-based monitoring, online monitoring based on wear debris is a primary method for acquiring real-time knowledge of a dynamic wear process as a direct indication of the wear condition. According to Dempsey and Afjeh *(2)*, the features of wear debris are more robust than vibration signals for operational influences and the ability to describe damage initiation and progression, especially in the early period. Therefore, approaches that adopt wear features are attracting more attention in machine monitoring (Roylance, et al. *(3)*). Various online methods for extracting information about wear have been proposed and they can be classified into three categories according to the different physical principles they use (Wu, et al. *(4)*; Miller and Kitaljevich *(5)*; Kwon, et al. *(6)*). Although these methods have been applied widely, our knowledge of wear particle characteristics is limited because they only use electrical signals to represent information pertaining to wear. However, the recently developed direct approaches that use imagery can provide more comprehensive information related to wear in order to characterize this information (Wu, et al. *(7)*).

Wear stages can be inferred from various parameters such as the wear rate, wear mechanism, and severity of wear. Of these possibilities, the wear rate using particle counting is one of the most frequently used indicators in many applications because the wear rate can be obtained from sensors such as the MetalScan sensor (Becker, et al. *(8)*). However, other indicators such as the size of debris also play a key role in determining the wear status, but they cannot be obtained from particle counting. In fact, wear is such a complicated process that it must be described collectively using the wear rate, wear mechanism, and wear severity (Peng and Kessisoglou *(9)*; Ludema *(10)*). An attempt to satisfy this need using online images of wear debris to determine the wear state from particle dimensions (Wu, et al. *(11)*) has recently been reported, but to

**CONTACT** Tonghai Wu wt-h@163.com
Color versions of one or more of the figures in the article can be found online at www.tandfonline.com/utrb.
Review led by Nick Weinzapfel.

## Nomenclature

$A_i =$ Particle coverage area in an image
$D =$ Average distance of all newly emerging samples
$D_L =$ Concentration of large wear particles
$D_S =$ Concentration of small particles
$G(\cdot) =$ Kernel function
$H =$ Bandwidth matrix
$h =$ Band width value
$I =$ Unit matrix
$L =$ Height of the object area
$Ne =$ Number of newly emerging data
$R^d =$ $d$-Dimensional space
$S^h =$ Initial spherical space with fixed center and radius $h$
$W =$ Width of the object area
$WS =$ Function of wear state
$w(\cdot) =$ Weighting coefficients for each sample
$\delta =$ Threshold

characterize particles with only information such as the coverage area may pose difficulties when the number and dimensions of the particles vary. For example, two pictures with the same particle coverage area may have different numbers of particles and dimensions, which may indicate different wear conditions. Later research solved this problem by extracting the individual features of particles using a statistical description and additional parameters (Wu, et al. *(12)*). This finding has enabled a more comprehensive characterization of wear debris and wear states.

When reliable information about the wear process has been acquired, a mathematical model of wear through the time domain can be constructed. Modeling the dynamic wear process is essential for online wear trend analysis. Analytical models based on the principle of asperity and Archard equations are widely used for such purposes (Meng and Ludema *(13)*). However, models that use contact mechanics focus on a transit time span and are referred to as microscales, so they are not directly applicable to machine wear processes at full life scale. Alternative approaches such as data-based methods that include threshold-based trend prediction and fuzzy modeling have advantages in modeling lifelong wear in off-line wear monitoring (García, et al. *(14)*; Zhang, et al. *(15)*; Peng and Zirk *(16)*). These methods extract the changes and trends from a large amount of data by clustering the salient features. The threshold method is the simplest and is mostly used for generating precaution alerts for ongoing faults. The trend method relies on gray theory and time series averaging and is also a popular choice in many applications. However, with all of these data-based models, the accuracy of the prediction is a primary problem in monitoring because they only rely on the mathematical features of data, and the wear deterioration mechanism is rarely included.

Intelligent methods have been developed to improve the qualities of the wear model. For instance, a model of a nonlinear system can be constructed by using machine learning techniques (Jian, et al. *(17)*), as well as artificial neural networks, but these methods require an indispensable training phase to make the model capable and vast reference samples that may be expensive or not available for a friction system in industry. In an effort to break the limitation of sample requirements, a support vector data description algorithm has proved that it can perform wear data clustering with less demand on samples, but it still requires normal data to construct the primary cluster model (Wu, et al. *(11)*). As a result, considering the absence of prior knowledge of wear progress for an unknown friction system, which is very general in industry, these methods are confined to online monitoring. To this end, free training samples and intelligent adaptabilities are deemed necessary to model and identify online wear states. Generally, the modeling strategy used to identify and describe the wear state should also include the following characteristics: (1) the wear mechanism should be included in the modeling strategy because it directly induces the development of failure and (2) because wear is regular over a long period but random over a short time, the model should not only identify data from different stages but should also adjust itself continuously throughout its full lifetime.

Aiming at a reliable characterization of the evolution of wear states, a new procedure that uses online wear particle imaging is formulated in this research. Firstly, to incorporate wear-related information with a description of the wear state, a static wear state is characterized quantitatively via the three features extracted from wear debris images. Secondly, a static binary-class model is developed with a machine learning algorithm to differentiate the wear datum from different stages. Thirdly, an improved adaptive dynamic method is built to identify and model the wear state transitions. Finally, the modeling strategy is verified via a four-ball machine wear test. This proposed method can identify the stages in a dynamic wear process that reveal the development of the wear state. This work provides a new and practical method for modeling the wear process with greater accuracy and also pushes the wear-based monitoring approach further in a condition-based monitoring application.

The rest of this article is organized as follows. The imaging system and the process for extracting information on wear are described in the following section. The definitions of the wear process indices are also given from a review of background works. The principle of the mean shift algorithm specialized for wear state modeling, including the procedures used to dynamically conduct and identify the wear state development, are presented in the next section. Finally, a conclusion to this work is drawn in the last section.

## Characterizing online wear information based on wear debris image

Only after the sensed information has been quantified can an intelligent technique be used to reduce the human influence in condition monitoring. Various mathematical indicators of wear have been proposed and applied, but most online wear monitoring techniques use particle counting to indicate the wear state for diagnostic and predictive purposes (Wu, et al. *(4)*). However, previous experience from analytical ferrography has revealed that describing a wear state using only the wear rate is not comprehensive, so other parameters such as the associated wear mechanism are used for a more profound characterization of wear (Wu, et al. *(11)*). On the other hand, severe wear that is used in traditional ferrography to indicate the degree of deterioration can also be used to characterize wear states. An improved method has been developed by integrating three indicators obtained from online images of wear particles (Wu, et al. (12); Wu, et al. (18)); these include the wear rate, percentage of large particles, and number of particles.

## Features of debris from online images of wear debris

In online ferrograph images, the agglomeration of wear particles will hamper the extraction of individual particle features. Therefore, the particle chains in the images were separated according to a segmentation strategy published previously (Wu, et al. (12)), allowing the extraction of individual wear particle features.

### Wear rate

The wear rate is a basic parameter for characterizing wear that has traditionally been used in many ferrography-based evaluations of the wear process (Lim, et al. (19)). An index of wear rate was formulated from images of online wear debris (Wu, et al. (20)) to represent the statistical coverage of wear debris in a defined area. The index of the particle coverage area (IPCA), denoted as $I$, is given by

$$I = \frac{A_i}{W \times L} \times 100\%, \qquad [1]$$

where $A_i$ is the particle coverage area in an image, and $W$ and $L$ are the width and height of the object area, respectively (Wu, et al. (7)).

### Percentage of large particles

According to conventional ferrography, the dimensions of the wear particles are primary indicators of the severity of wear, where variations in this index often indicate the severity of the wear process. Generally, wear debris in the captured image contains both large wear debris and small debris. However, the quantity of small debris increases continuously with operating time. A sharp rise in the quantity of large debris indicates abnormal wear. In addition, the existence of large wear debris will also lead to imminence of catastrophic failure due to the phenomenon of three-body wear. Therefore, another important indicator of the wear process, the percentage of large particles (PLP), denoted as $P$, is also used in this work (Goncalves and Campos (21)). We have

$$P = \frac{D_L - D_S}{D_L + D_S} \times 100\%, \qquad [2]$$

where $D_L$ is the number of large wear particles in the captured image (i.e., $>30\ \mu$m) and $D_S$ is the number of small particles in the captured image (i.e., $<30\ \mu$m). Experiments revealed that if two images have the same IPCA, their corresponding PLP can be very different, so it can be stated that these two parameters have decoupled in describing the wear process, and their integration improves the reliability of this characterization.

### Number of particles

The number of wear particles (NUM), denoted as $N$, is another important index that is widely used to monitor the wear condition of running machines (Goncalves and Campos (21)); indeed, it is often used to indicate the wear rate and the accompanying particle size. In this proposed wear characterization system, the indices IPCA and NUM are used in conjunction and are obtained from the image particle separation method suggested in Wu, et al. (18).

### Wear state characterization

Using the three indices described above, a comprehensive model to characterize the wear state is developed. This model, denoted as $WS$, is given by

$$WS = f(I, N, P). \qquad [3]$$

Unlike the current counterparts, it will describe the wear mechanism more accurately because it contains more information about the wear debris.

The wear state can thus be described quantitatively by a function of the three parameters. Furthermore, by extracting these indices from the online images of wear debris, the wear performance at different states can be identified and a lifelong wear process can be characterized.

## Experimental application of wear state characterization

To examine the proposed method, an experimental application is carried out with a four-ball wear test rig, as shown in Fig. 1.

As Fig. 1 shows, a four-ball tribosystem is used to generate wear particles under specific loads and rotation speeds. The test ball utilized in this experiment is bearing steel ball that is manufactured of carbon chromium bearing steel (GCr15), with surface roughness of 0.025 mm and hardness in the range 58–63 HRC. Wear particles are collected by the oil cup and circulate with the lubricant driven by a digital pump. An online visual ferrograph (OLVF) sensor is placed in the oil circulation path to collect wear debris for imaging. After being captured and imaged, all of the particles are removed from the flow. These particles are filtered with a magnetic tube and thus would not circulate with oil, which ensures that each wear particle analyzed by the OLVF sensor is freshly produced from the wear process.

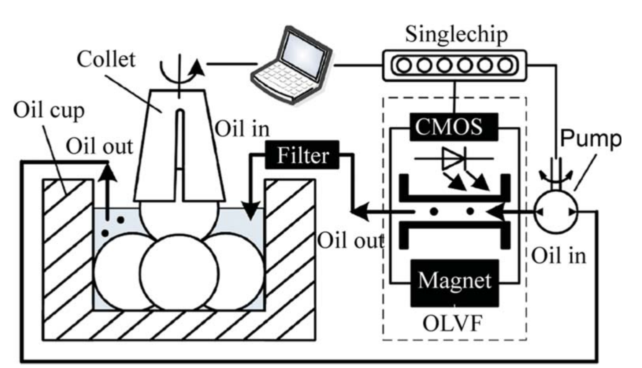


Figure 1. Schematic diagram of the four-ball test rig with online wear particle monitoring.

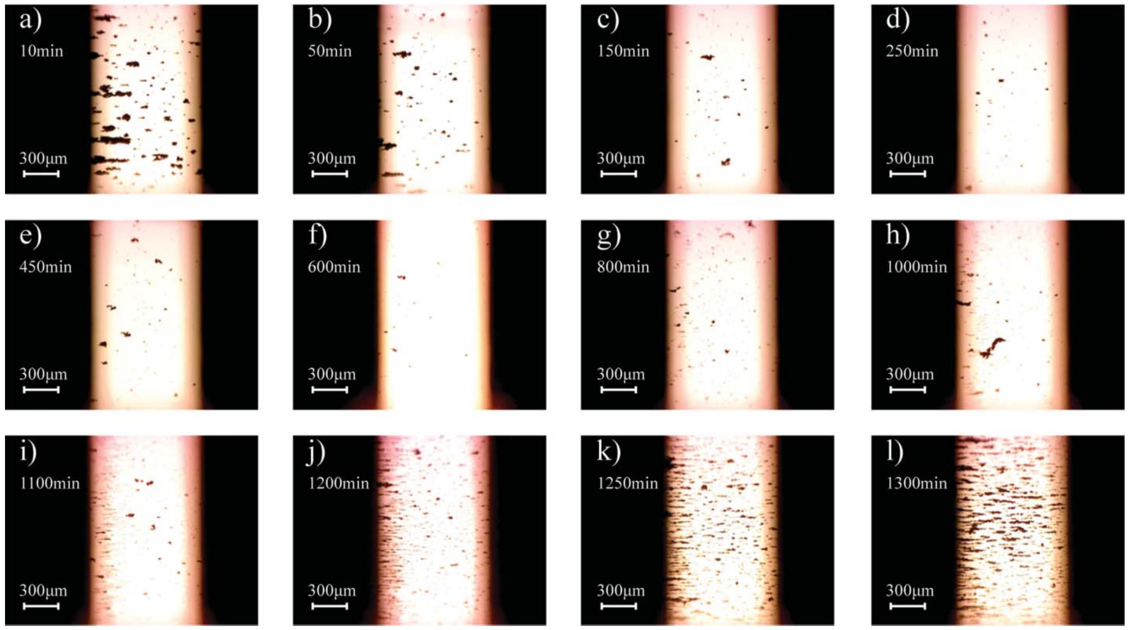


**Figure 2.** Images of wear debris from a four-ball wear test taken at different times: (a) 10 min, (b) 50 min, (c) 150 min, (d) 250 min, (e) 450 min, (f) 600 min, (g) 800 min, (h) 1,000 min, (i) 1,100 min, (j) 1,150 min, (k) 1,200 min, and (l) 1,250 min.

An experiment was carried out for 20 h at a constant speed of 500 rpm. To simulate a degrading wear process, a load of 1,500 N was applied for the first 800 min and a load of 2,000 N was applied for the remaining time. Some typical images of wear debris at different time instances are shown in Fig. 2; these images revealed that the amount of wear debris varied with the test duration. According to this information, a developing trend of wear state, including severe wear, normal wear, and further severe wear, can be roughly identified manually, but there are explicit differences in the size of particles in the two cases of severe wear. The wear particles in initial running wear are generally larger than those in the final one, so there are generally, but not necessarily, three typical stages in a full wear process. These stages are running-in, normal, and severe (Kothamasu, et al. *(1)*), and they can be clearly seen in the test results shown in Fig. 2.

By adopting the techniques used in previous works (Wu, et al. *(12)*; Wu, et al. *(18)*), three indices for characterizing the wear rate, degree of wear, and severity of wear were extracted from each image. The time history of each indicator is shown in Fig. 3, where these indicators will be normalized to facilitate comparisons in the following part. Figures 3a and 3b show that the IPCA and NUM indices are positively correlated in their general trend. Both indices also show three stages in the testing duration of 1,250 min, which is consistent with the state features observed from Fig. 2. Moreover, both indicators have higher values in the final stage than in the initial stage, and the debris in Figs. 2j–2k indicates more severe wear than that in Figs. 2a–2c. This observation also agrees with a generally reported phenomenon that wear in the severe stage is greater than that in the running-in stage, although both stages exhibit high wear rates (Kothamasu, et al. *(1)*). Furthermore, the change in load at 800 min is intuitively identifiable from both indicators, though the variations in the two indices are not identical. At 800 min, a dramatic change occurs in IPCA but only a slight fluctuation can be identified from NUM. However, a corresponding increase is found from PLP, which means that there is an increase in the amount of large particles at this time.

The above comparison between the proposed method and the intuitive observation indicates that wear states with various mechanisms can be represented by the proposed indicators, and with such a mathematical representation, a promising prospect can be expected for an automatic online identification of a wear process. Based on this motivation, a model has been developed to automatically identify the wear states, and it is described in the following section.

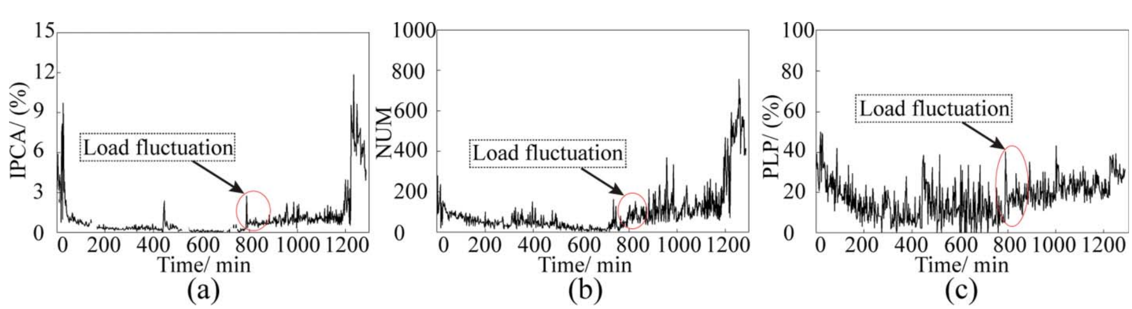


**Figure 3.** Variations in different indicators in the wear process of a four-ball test: (a) IPCA, (b) NUM, and (c) PLP.

## Wear state modeling with proposed indices

Wear is a process with continuous and gradual features, as described by a bathtub-shaped curve in which several "stages" exist. The data samples show similar features in the same stage due to similar wear mechanisms. Identifying the wear state is actually a process of assembling data with similar features. To overcome the problem encountered by the current modeling, as mentioned in the Introduction, a basic clustering method is used to categorize wear states by referring to the three proposed indices. Firstly, a static model to identify wear data would be used to prove the effectiveness of the model, followed by online monitoring to identify the wear data dynamically. A dynamic self-adapting strategy that focuses on determining the transition between the two states is investigated so that a dynamic wear state model for online monitoring can be constructed from a series of wear states identified from online images. Finally, the method is verified with the data sampled from the bench test, as shown in Fig. 1.

### *Principle of mean shift–based modeling*

A mean shift is a nonparametric approach to modeling that uses the probability of density but not previous samples. The objective of a mean shift algorithm is to cluster a set of input samples into different categories with identified centers where data from the same category share the same convergence center. The fundamentals of mean shift–based identification modeling can be explained as follows.

Suppose a $d$-dimensional space contains $n$ variables; that is, $[x_1, \ldots, x_n] \in R^{dn}$, we can define a vector $M_h$ as

$$M_h(x) = \frac{1}{k}\sum_{x_i \in S_h} (x_i - x), i = 1, \cdots, n, \qquad [4]$$

where $x_i$ is a set of the points chosen from an initial spherical space $R^d$ centered at $x$ with radius $h$. The vector $M_h(x)$ is the mean distance of all of the $k$ samples falling within $S_h(x)$ to the center $x$.

A kernel function $G(x)$ is introduced by allowing a weighted coefficient for each sample on the basis of its distance from the center, so a mean shift function can be written as

$$M_h(x) = \frac{\sum_{i=1}^{n} G_H(x_i - x) w(x_i)(x_i - x)}{\sum_{i=1}^{n} G_H(x_i - x) w(x_i)}, \qquad [5]$$

where

$$G_H(x_i - x) = |H|^{-1/2} G\left(H^{-1/2}(x_i - x)\right). \qquad [6]$$

Here, $H$ is the matrix of the bandwidth, which represents the initial radius of the spherical space, and $w(x_i)$ are weighting coefficients for each sample $x_i$.

For simplicity, the bandwidth matrix H is often defined as a diagonal matrix that takes the form $H = h^2 I$ where $I$ is a unit matrix. Therefore, Eq. [5] can be transformed into

$$M_h(x) = \frac{\sum_{i=1}^{n} G_H\left(\frac{x_i - x}{h}\right) w(x_i) x_i}{\sum_{i=1}^{n} G_H\left(\frac{x_i - x}{h}\right) w(x_i{}^{i})} - x, \qquad [7]$$

which can be simplified as

$$M_h(x) = m_h(x) - x, \qquad [8]$$

where $m_h(x)$ is

$$m_h(x) = \frac{\sum_{i=1}^{n} G_H\left(\frac{x_i - x}{h}\right) w(x_i) x_i}{\sum_{i=1}^{n} G_H\left(\frac{x_i - x}{h}\right) w(x_i)}. \qquad [9]$$

Given an arbitrary starting point $x$, a kernel function $G(x)$, and a threshold $\delta$, a three-step iteration can be implemented as follows:

1. Calculate the value of $m_h(x)$ with Eq. [9].
2. Terminate if $|m_h(x) - x| < \delta$; else repeat step 1.
3. Update $x = m_h(x)$.

After completing this process, all of the simple data will converge into a final center where data sharing the same center would be identified as samples from the same stage.

Determined as the clustering principle of the mean shift–based method, effective identification theory varies when the data sample changes, so for static samples, only one iteration is needed to finish the clustering but for the dynamical samples where typically a set of samples with continuous data is involved, a new round of clustering should be conducted if the new samples are joined. These two clustering approaches will be explained.

### *Mean shift–based modeling for identifying the static wear state*

The key of the mean shift model for categorizing static wear states has two aspects: kernel function construction and bandwidth selection.

#### *Choice of kernel function*

The kernel function provides the weights for different data samples. There are several candidates for kernel functions such as uniform function and Gaussian function (Comaniciu and Meer *(22)*). Gaussian functions perform well on both the convergence rate and weight assignment of distributed sample points (Guo, et al. *(23)*), so the Gaussian kernel function is used in the wear modeling system because it adapts very well to sample numbers and dimensions. It takes the form of

$$K(x_i, x) = \exp\left(\frac{-|x_i - x|^2}{2h^2}\right). \qquad [10]$$

#### *Determination of bandwidth*

A smaller bandwidth will introduce more clusters and vice versa (Comaniciu *(24)*). The effects of bandwidth on the category results are shown in Fig. 4.

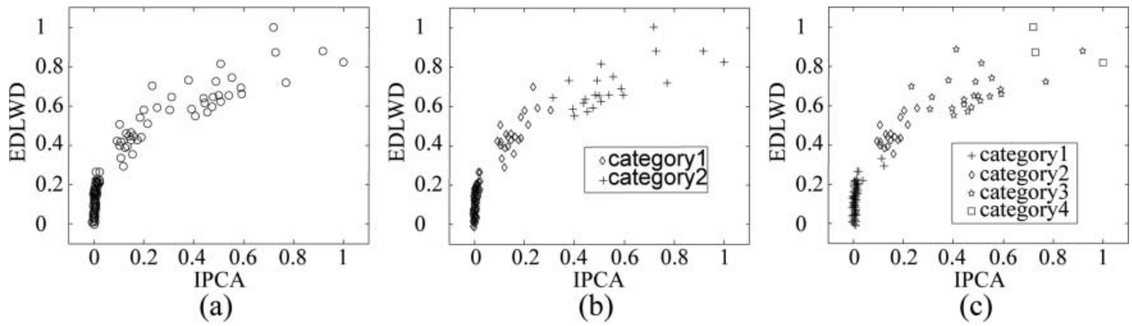


Figure 4. Effects of the choice of bandwidth on state identification: (a) initial 100 wear data from monitoring an engine, (b) clustering result with bandwidth = 0.3, and (c) clustering result with a bandwidth = 0.2.

A total of 100 wear data points from an engine bench test (Wu, et al. *(11)*) are clustered by the mean shift algorithm with different bandwidths. This bench test was conducted on a four-cylinder gasoline engine. Magnetic synthetic engine oil was utilized for lubrication. The temperature of lubrication was controlled around 95°C with a thermostat. The images of wear debris were captured via an OLVF that was installed in the bypass of the lubrication circulation. Two statistical indicators, the equivalent diameter of large wear debris (Wu, et al. *(11)*) and IPCA, are used to describe the wear data. Figures 4b–4c show that the number of clusters is enhanced when the bandwidth is reduced.

### *Static wear state identification*

A static identification of distinct types of wear data is the key requirement for a dynamic identification of the wear state, so to help with presentation, nine representative images were chosen from the wear process, as shown in Fig. 5.

By referring to a typical bathtub-shaped curve of the wear process, the images in Figs. 5a–5c are from the running-in stage, those shown in Figs. 5d–5f are from the stable stage, and images in Figs. 5g–5i are from the severe stage.

The three indicators IPCA, NUM, and PLP extracted from the imaging subsystem were normalized and plotted in a three-dimensional coordinate system, as shown in Fig. 6a. The mean shift model was constructed to obtain clusters of the example samples. Here, the bandwidth was set at 0.5, and a uniform kernel function was used to calculate the mean shift vector. After the iterations, three converging centers were located and marked in Fig. 6b with red circles. Each center represents a cluster of data with statistically identical features for the three

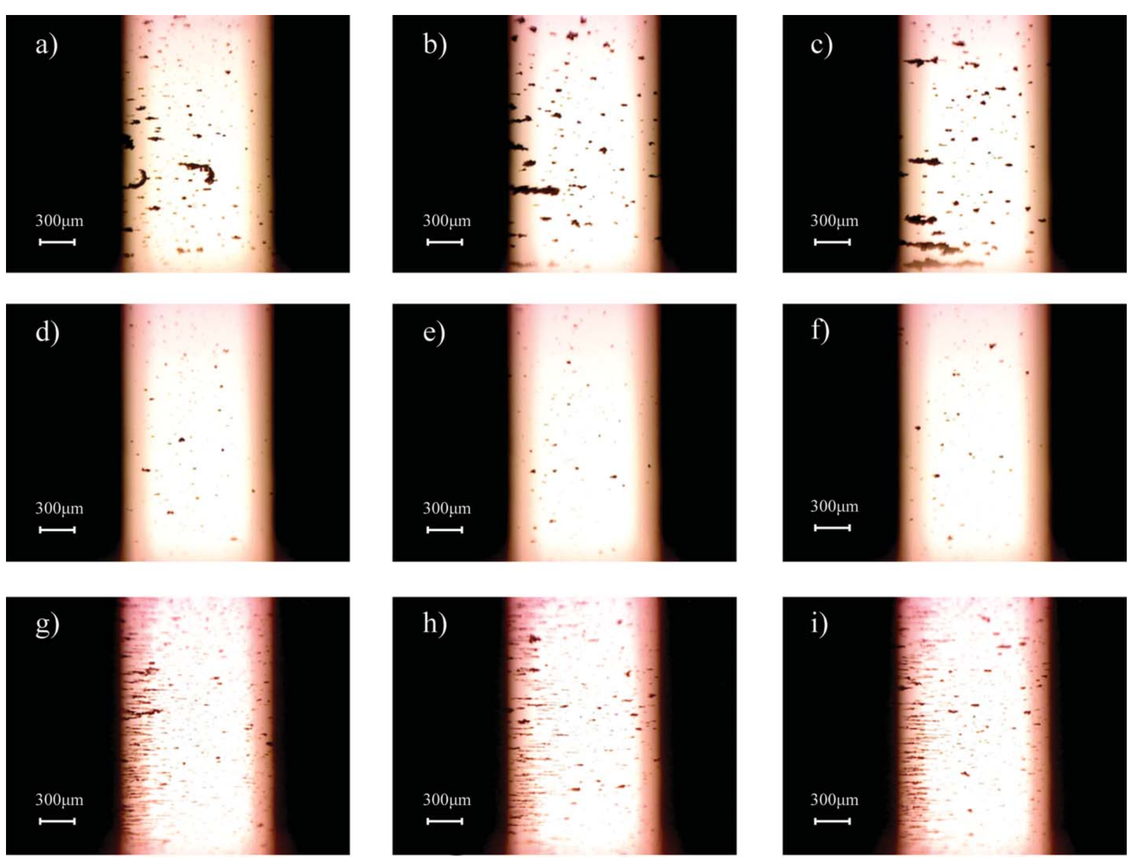


Figure 5. Images of representative wear debris in different stages: (a)–(c) running-in stage, (d)–(f) normal wear stage, and (g)–(i) severe wear stage.

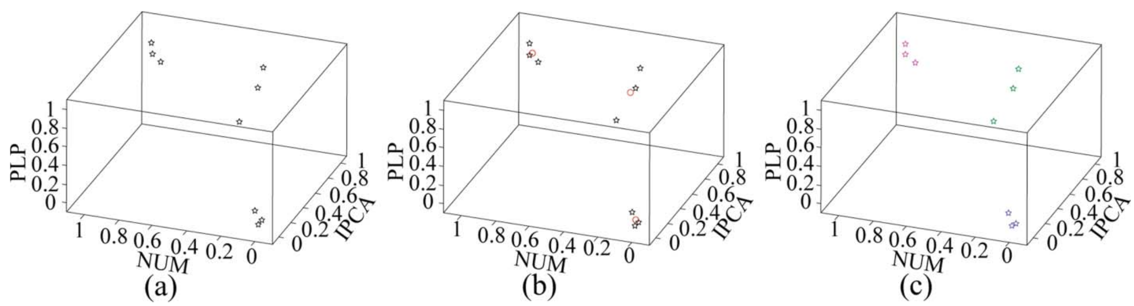


**Figure 6.** Wear state clustering by mean shift–based modeling method: (a) normalized wear data, (b) mean shift clustering, and (c) state identification.

indicators. Data sharing the same converging center are grouped as one cluster. The final clustering result is shown in Fig. 6c.

Three clusters were identified from the wear data provided, which agreed with the result from a qualitative inspection. The categories of each initial image data are shown in Table 1.

As a probability-based nonparametric method of estimation, the mean shift algorithm shows its superiority in robustness while dealing with highly random wear process data, but its reliability still depends on the choice of bandwidth. For a given static process data, a predefined bandwidth can be accomplished by tentative measurements. In summary, this method can identify wear samples from different states, but for dynamic modeling such as online monitoring, a constant predefined bandwidth is not suitable.

## Dynamically modeling wear state evolution by adaptive mean shift method

During real-time monitoring, the data set changes constantly due to continuous incoming samples, so a dynamic modeling approach to identify the wear state is needed. A dynamic wear process consists of several stages with relatively steady features in narrow time slots where being able to identify these wear stage transitions is necessary in order to model the wear process. Consequently, a dynamic adaptive mean shift identification model has been developed.

### Adaptive mean shift method

Practically speaking, dynamically modeling a wear process is used to identify the current stage and determine a new stage, so a binary-class method is needed here. Though online samples appear randomly, wear state samples under a dominant wear mechanism are essentially similar, which means that wear state samples can be categorized into different stages according to their similar mechanisms. With regards to the diversity of wear stages in the whole process, an adaptive model is needed to identify each stage by automatically adapting the model parameters to cope with the incoming samples.

**Table 1.** State categories of the object images in Fig. 5 identified by the mean shift.

| Images in Fig. 5 | (a) | (b) | (c) | (d) | (e) | (f) | (g) | (h) | (i) |
|---|---|---|---|---|---|---|---|---|---|
| Categories | 1 | 1 | 1 | 2 | 2 | 2 | 3 | 3 | 3 |

In a typical wear process, the wear rate and particle size are very diverse in the running-in and severe wear stages but have a relatively serried distribution in the normal state. Accordingly, when modeling the dynamic wear state process, the sparseness of data at different stages varies and a fixed bandwidth will create large errors in the results. Therefore, an adaptive bandwidth is needed to identify the developing wear processes; this means that the model should adjust its parameters and bandwidth dynamically to cope with fluctuations in the wear data. A data distribution–based adaptive bandwidth method was proposed by using a small bandwidth in dense distribution and a large bandwidth in sparse distribution (Comaniciu and Meer *(22)*), but this method means that a calculation must be carried out whenever a new data center is formed, and that would waste a large amount of computational resources. A simplified method is therefore proposed to identify the wear stages online.

The criterion for determining the bandwidth of a newly identified stage is such that when a data category transits to a new state, the average distance of these samples is calculated with the following equation by using the newly emerged data, such that

$$D = \frac{1}{C_{N_e}^2}\left(\sum_{i=1}^{Ne}\sum_{j=1}^{Ne} | x_i - x_j |\right), \qquad [11]$$

where $D$ denotes the average distance of all newly emerging samples. The variable $Ne$ denotes the number of emerged data. Accordingly, a new and incoming sparse distribution would introduce a large bandwidth and vice versa. The adaptive bandwidth would change automatically according to the distribution density of the samples obtained initially and would then remain constant until another state is identified.

A sketch of an adaptive loop of the dynamic model is shown in Fig. 7. This loop is designed to determine when a new state has come and where all data in online sampling generally fall into either normal or abnormal states. The loop is stopped until an increasing trend of abnormal samples is suddenly identified, and this indicates that a new state can be determined by all of the candidates. In each loop, a static mean shift algorithm is used to categorize all of the candidate samples into two types; this categorization is repeated when the candidates are renewed by a new incoming sample. A transition in the wear state is regarded as occurring once a loop has stopped.

Specifically, the number of candidate samples is recorded as *Num_data* and normal and abnormal samples are

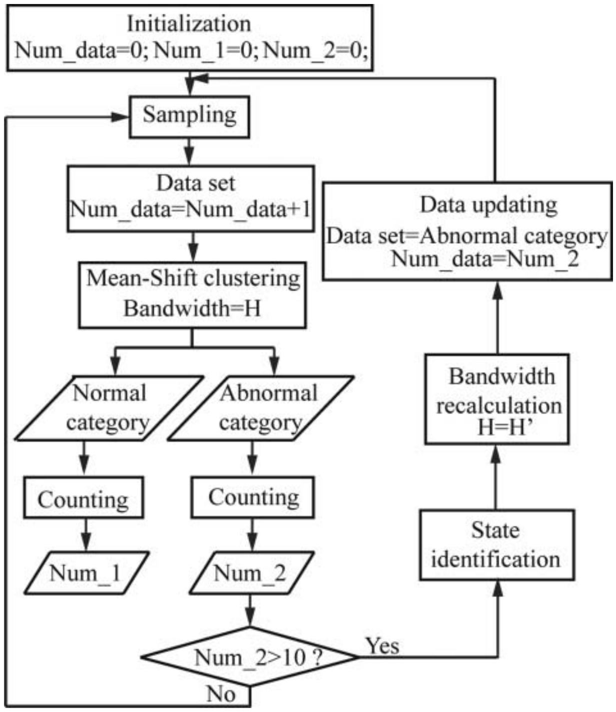


Figure 7. Flowchart of a dynamic mean shift clustering process.

denoted as *Num_1* and *Num_2*, respectively. At the beginning of the loop the variables *Num_data, Num_1*, and *Num_2* are initiated to zero, and the value of *Num_data* increases by one in the case of a new sample. The initial point is the first sample in a sequence and it is set as a normal sample. Then the mean shift model with a fixed bandwidth $h$ starts to categorize all of the candidate samples and the numbers of abnormal and normal categories are counted. If the condition where $Num\_2 > 10$ is satisfied, a new wear state is identified with all normal samples and those abnormal samples are carried into the next loop as initial candidates. A new bandwidth is then calculated and these initial candidates are adapted to the new wear state.

## *Monitoring the wear state with the adaptive mean shift model*

Having completed the dynamic modeling strategy for identifying the wear state, the wear data obtained in the four-ball wear test are processed to perform an online simulation. All of the wear data contained in the three indictors are input into the model one by one to imitate the online sampling process. The mean shift model starts its calculation loop when each new sample appears and determines a new wear state once the condition is satisfied. Each wear state identified is marked as a cluster, and with the increasing number of wear states in time, the development of wear can be inferred. Figure 8 illustrates the overall dynamic process of wear state identification with a three-dimensional space composed of PLP, NUM, and IPCA. As the number of input data increases continuously, adjacent wear states are identified.

Figure 8 shows that the state center and sparseness of samples vary as the states develop. At the beginning of the monitoring period, after five samples are categorized as the normal state, a new state emerges, as shown in Figs. 8a–8b. These categorized samples are then removed and the identification process continues, as shown in Figs. 8b–8c. A new state transition is identified and a new data cluster emerges. Similarly, state transitions also appear in the following groups as Figs. 8c–8d and Figs. 8d–8e. To summarize, transitions in the wear state are identified dynamically as the samples are continuously incoming but note that the bandwidth adapts to cope with different states because it first experiences a decrement and then increases, as shown in Fig. 9; this coincides with a typical sequence of severe wear, normal wear, and severe wear.

To illustrate the overall development of wear stages over its life span, the stage transitions are plotted together with variations in the bandwidth against the time axis as the value of $b$ shown in Fig. 9. Intuitively, the whole process consists of four wear states with the transition times and corresponding bandwidths. More detailed information can be extracted as follows.

In this figure where the first state is marked with a red circle, it is very transitory, so it is combined with the adjacent state as

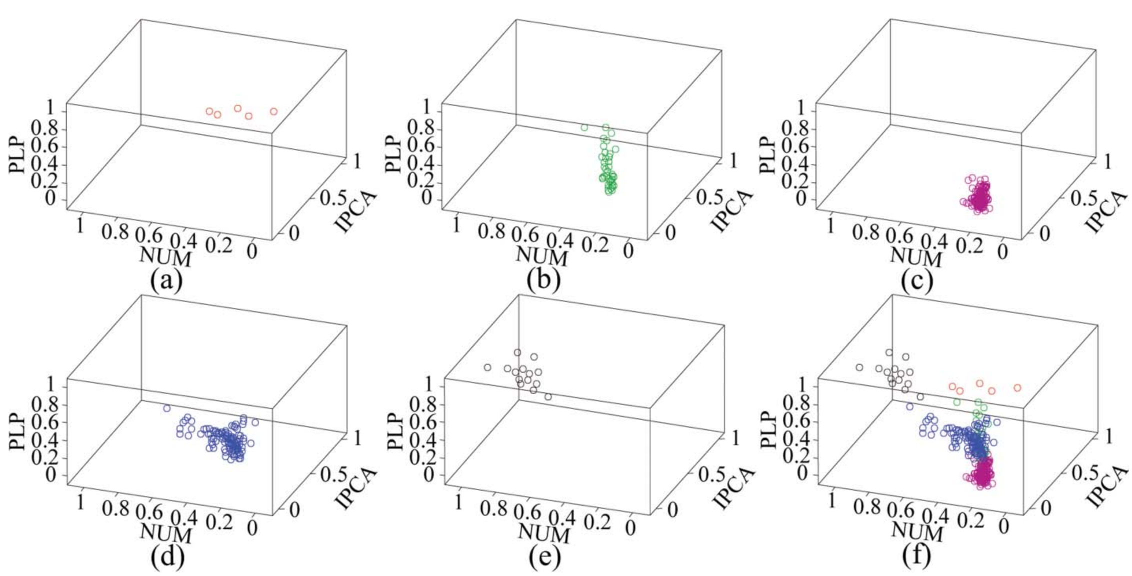


Figure 8. Identifying the wear stage with dynamic mean shift modeling: (a) initial stage, (b) second stage, (c) third stage, (d) fourth stage, (e) last stage, and (f) overall stages.

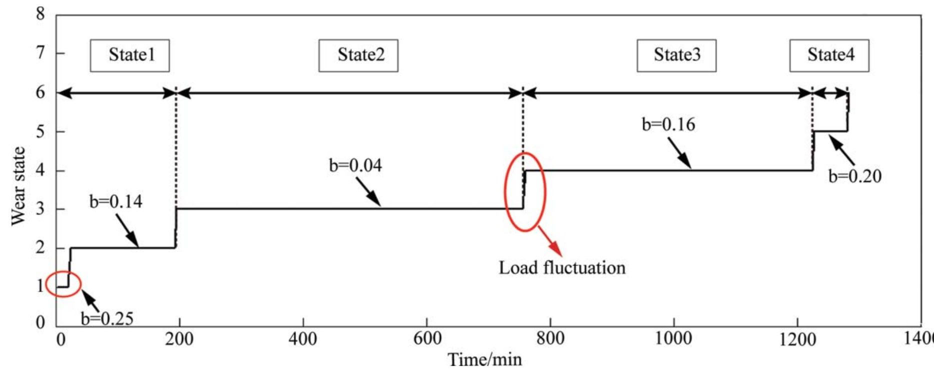


**Figure 9.** Overall development of wear stages in a full wear process.

state 1, which is the initial wear state. During the 1,250 min of running time, the running-in state accounts for about 200 min, with 20 min in the initial stage and 180 min in the transition to a new state. At around 800 min, the load changes from 1,500 to 2,000 N and, correspondingly, a new wear state transition is identified as a response to further wear; after 1,200 min, a severe wear state is reached. This observation reveals that more wear states have been identified as well as the typical three-phase wear process. The reason is that a wear state transition is not only an indicator of natural wear but is also the result of operating conditions.

Wear debris is generated directly from friction between the two tribopair surfaces, features that can indicate that wear has accumulated in the machine. On this basis, surface information of the tribopair can be utilized as a parallel indicator and as debris information to describe the wear state. The mean shift–based modeling strategy has proved capable of identifying the wear state transition over a full lifetime, including information on wear debris. However, the transition state is the result of mathematical modeling, so to make this method more convincing, a repetitive experiment is necessary.

As mentioned before, four wear states were identified and the wear debris showed distinct features in different wear states; accordingly, the wear surfaces will show different characteristics. For the purpose of verification, four friction tests on the same four-ball machine and same load condition were conducted to obtain specific information about the surfaces of the four corresponding wear states with specific test times. Moreover, experiments conducted over 2, 10, 15, and 21 h were repeated. Information regarding the surfaces of the upper and lower balls was collected by laser scanning confocal microscopy (LSCM), as shown in Fig. 10. For simplification, only pictures of one lower ball among each three were utilized. Figures 10a–10d are LSCM images of the wear scar from the upper ball, and Figs. 10e–10h are images of the lower ball.

As Fig. 10 shows, the scars on the upper and lower balls due to wear have distinct features at different stages; in the first stage, which refers to Figs. 10a and 10e, the diameter of the wear area is only 1 mm, and there is an unworn area in the wear area and the width of the scratch is remarkable; these are typical features of the running-in stage. In the second stage, which refers to Figs. 10b and 10f, the diameter of the wear area has increased to 1.2 mm, there is no unworn area, and the

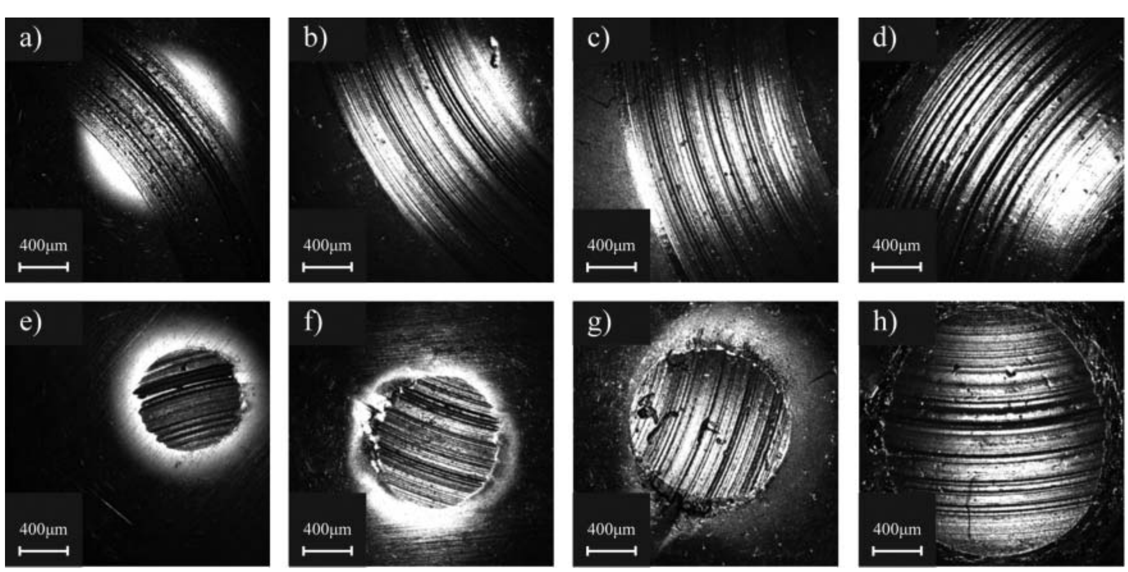


**Figure 10.** LSCM images of the surfaces of balls from different states: (a) surface of upper ball after 2 h, (b) surface of upper ball after 10 h, (c) surface of upper ball after 15 h, (d) surface of upper ball after 21 h, (e) surface of lower ball after 2 h, (f) surface of lower ball after 10 h, (g) surface of lower ball after 15 h, and (h) surface of lower ball after 21 h.

scratches are thinner than in the first stage, which means that the running-in stage is over and a new normal stage is beginning. In the third stage after the load has increased (Figs. 10c and 10g), the diameter of wear area has increased to 1.6 mm, and the scratch is more serried than the former one. In the fourth stage, which refers to Figs. 10d and 10h, the diameter of wear has increased to 2.4 mm and the scratches are sparse but deeper and wider than in the former stage.

According to the LSCM images from four-ball tests carried out with different time lengths and workloads, the surfaces of the four balls were identified by mean shift modeling at different stages and indicated distinct features and distinguishing wear mechanisms. Therefore, the mean shift–based modeling method can identify different wear states over the full lifetime of a machine.

In summary, dynamic identification modeling can monitor the natural transition of wear states and the transition states due to changes in the working conditions. When this online debris data are acquired, the wear mechanism transition can be automatically described as being in a mathematical format, which makes the use of artificial intelligence applicable. As a result, there will be less dependence on human experience and techniques and therefore this can be regarded as a practical and reliable approach for monitoring wear-based conditions.

## Conclusions

Wear states consisting of a full wear process and the development of these wear states were reflected by the gradual degradation of machine performance. A mathematical characterization of these dynamic variations was investigated for monitoring the health of machines online. This article has focused on characterizing the health of machines based on their wear mechanism and then constructing a strategy to dynamically identify and monitor wear states in real time. Three wear indicators, including the percentage of area covered, number of particles, and larger particle ratio of wear debris, were utilized to digitalize the wear state. Additionally, a mean shift–based identification model was constructed to quantitatively classify and determine particular wear state transitions over the full lifetime of a machine. Finally, the model was verified with a set of wear debris images acquired from a four-ball wear experiment. By imitating an online sampling process with the wear data, a detailed wear state transition and development was dynamically identified. The corresponding distinct wear mechanism was also verified via LSCM images. This modeling method can provide a new method to monitor wear online based on evaluating the development of wear over the life span of a machine.

However, this method cannot be regarded as a versatile strategy for wear monitoring of machinery systems due to its limitation in mechanism interpretation. Further work will be conducted to make this work more industrially applicable.

Online monitoring requires all of the calculations to be manually independent. However, adaptive as the bandwidth is in this article, a manual initialization of bandwidth toward specific monitored machines is necessary to start iteration. Intelligent theory can be involved to make this method more robust in different situations.

Because debris images are a source of the origin of wear information, accurate extraction of wear debris features is critical for reliable monitoring of the wear condition. However, due to the limited resolution of the Complementary Metal Oxide Semiconductor (CMOS), the performance of the debris sensor is still unsatisfactory when the size of the wear debris is too small. For a precision tribopair or mild wear, it is hard to extract precise condition information. Therefore, hardware amelioration should be conducted in future work.

## Acknowledgement

The author acknowledges all of the members of the Tribology Research Group in the School of Mechanical & Manufacturing Engineering, the University of New South Wales, for very helpful discussions.

## Funding

Financial support for the present research was provided by the National Science Foundation of China (Grant Nos. 51275381, 50905135) and Fundamental Research Funds for the Central Universities of China.

## ORCID

Ngaiming Kwok http://orcid.org/0000-0002-5430-6860

## References

(1) Kothamasu, R., Huang, S. H., and VerDuin, W. H. (2009), *Handbook of Maintenance Management and Engineering*, 1st ed., Springer: London.
(2) Dempsey, P. J. and Afjeh, A. A. (2004), "Integrating Oil Debris and Vibration Gear Damage Detection Technologies Using Fuzzy Logic," *Journal of the American Helicopter Society*, **49**(2), pp 109–116.
(3) Roylance, B. J., Williams, J. A., and Dwyer-Joyce, R. (2000), "Wear Debris and Associated Wear Phenomena Fundamental Research and Practice," *Proceedings of the Institution of Mechanical Engineers - Part J: Journal of Engineering Tribology*, **214**(1), pp 79–105.
(4) Wu, T. H., Wu, H. K., Du, Y., and Peng, Z. X. (2013), "Progress and Trend of Sensor Technology for On-Line Oil Monitoring," *Science China Technological Sciences*, **56**(12), pp 2914–2926.
(5) Miller, J. L. and Kitaljevich, D. (2000), "In-Line Oil Debris Monitor for Aircraft Engine Condition Assessment," *IEEE Aerospace Conference Proceedings*, 25 March, Montana, US.
(6) Kwon, O. K., Kong, H. S., Han, H. G., Yoon, E. S., Myshkin, N. K., Markova, L. V., and Seneniouk, M. S. (2000), "On-Line Measurement of Contaminant Level in Lubricating Oil," **U.S. Patent 6,151,108**.
(7) Wu, T. H., Mao, J. H., Wang, J. T., Wu, J. Y., and Xie, Y. B. (2009), "A New On-Line Visual Ferrograph," *Tribology Transactions*, **52**(5), pp 623–631.
(8) Becker, A., Abanteriba, S., and Forrester, D. (2015), "Determining Inductive Sensor Wear Debris Limits for Rolling Contact Fatigue of Bearings," *Proceedings of the Institution of Mechanical Engineers - Part J: Journal of Engineering Tribology*, **229**(6), pp 698–711.
(9) Peng, Z. and Kessissoglou, N. (2003), "An Integrated Approach to Fault Diagnosis of Machinery Using Wear Debris and Vibration Analysis," *Wear*, **255**(7), pp 1221–1232.
(10) Ludema, K. C. (1996), "Mechanism-Based Modeling of Friction and Wear," *Wear*, **200**(1), pp 1–7.
(11) Wu, T. H., Peng, Y. P., Wu, H. K., Zhang, X. G., and Wang, J. Q. (2014), "Full-Life Dynamic Identification of Wear State Based on On-Line Wear Debris Image Features," *Mechanical Systems and Signal Processing*, **42**(1), pp 404–414.
(12) Wu, T. H., Wu, H. K., Du, Y., Kwok, N., and Peng, Z. X. (2014), "Imaged Wear Debris Separation for On-Line Monitoring Using

Gray Level and Integrated Morphological Features," *Wear*, **316**(1), pp 19–29.

*(13)* Meng, H. C. and Ludema, K. C. (1995), "Wear Models and Predictive Equations: Their Form and Content," *Wear*, **181**, pp 443–457.

*(14)* García, F. P., Tobias, A. M., Pinar, J. M., and Papaelias, M. (2012), "Condition Monitoring of Wind Turbines: Techniques and Methods," *Renewable Energy*, **46**(5), pp 169–178.

*(15)* Zhang, H., Li, Z., and Chen, Z. (2003), "Application of Grey Modeling Method to Fitting and Forecasting Wear Trend of Marine Diesel Engines," *Tribology International*, **36**(10), pp 753–756.

*(16)* Peng, Z. and Kirk, T. B. (1999), "Wear Particle Classification in a Fuzzy Grey System," *Wear*, **225**(4), pp 1238–1247.

*(17)* Jian, W., Dong, Y., Hu, D. X., Zao, J. J., and Peng, B. (2013), "Application of Relevance Vector Machine in the Engine Oil Wear Particle Fault Diagnosis," *2nd International Symposium on Instrumentation and Measurement, Sensor Network and Automation (IMSNA)*, Toronto, Canada, 23–24 December.

*(18)* Wu, H. K., Wu, T. H., Peng, Y. P., and Peng, Z. X. (2014), "Watershed-Based Morphological Separation of Wear Debris Chains for On-Line Ferrograph Analysis," *Tribology Letters*, **53**(2), pp 411–420.

*(19)* Lim, S. C., Ashby, M. F., and Brunton, J. H. (1987), "Wear-Rate Transitions and Their Relationship to Wear Mechanisms," *Acta Metallurgica*, **35**(6), pp 1343–1348.

*(20)* Wu, T. H., Wang, J. Q., Wu, J. Y., Xie, Y. B., and Mao, J. H. (2011), "Wear Characterization by an On-Line Ferrograph Image," *Proceedings of the Institution of Mechanical Engineers - Part J: Journal of Engineering Tribology*, **225**(1), pp 23–34.

*(21)* Goncalves, A. C. and Campos, J. B. (2011), "Predictive Maintenance of a Reducer with Contaminated Oil under an Excentrical Load through Vibration and Oil Analysis," *Journal of the Brazilian Society of Mechanical Sciences and Engineering*, **33**(1), pp 1–7.

*(22)* Comaniciu, D. and Meer, P. (2002), "Mean Shift: A Robust Approach toward Feature Space Analysis," *IEEE Transactions on Pattern Analysis and Machine Intelligence*, **24**(5), pp 603–619.

*(23)* Guo, S. M., Chen, L. C., and Tsai, J. S. H. (2009), "A Boundary Method for Outlier Detection Based on Support Vector Domain Description," *Pattern Recognition*, **42**(1), pp 77–83.

*(24)* Comaniciu, D. (2003), "An Algorithm for Data-Driven Bandwidth Selection," *IEEE Transactions on Pattern Analysis and Machine Intelligence*, **25**(2), pp 281–288.